Electronic Supplementary Material (ESI) for Journal of Materials Chemistry C.
This journal is © The Royal Society of Chemistry 2024

# Supporting Information

# Effect of Sn Valence State in situ-growth of FeOOH Precursor on Performance of α-$Fe_2O_3$ Photoanode

Weiwei Xia[a*], Zichun Chai[Ŧa], Rui Zhang[a], Junhui He[a], Xianghua Zeng[a,b*]

[a] *College of Physics Science and Technology & Institute of Optoelectronic Technology, Yangzhou University, Yangzhou 225002, P.R. China*

[b] *College of Electrical, Energy and Power Engineering, Yangzhou University, Yangzhou 225127, P. R. China*

## Supporting Information

- **Results and discussion**

**Figure S1.** Tauc's plots of the synthesized $Fe_2O_3$, $Sn^{2+}$-$Fe_2O_3$ and $Sn^{4+}$-$Fe_2O_3$ films.

Table S1. Relative percentage of Sn for $Fe_2O_3$, $Sn^{2+}$-$Fe_2O_3$ and $Sn^{4+}$-$Fe_2O_3$ films.

| | Fe | O | Sn |
|---|---|---|---|
| Samples | At% | At% | At% |
| $Fe_2O_3$ | 24.07 | 75.93 | * |
| $Sn^{2+}$-$Fe_2O_3$ | 20.82 | 68.74 | 10.44 |
| $Sn^{4+}$-$Fe_2O_3$ | 21.45 | 77.90 | 0.65 |

Table S2. Relative percentage of $O_L$ and $O_V$ components for $Fe_2O_3$, $Sn^{2+}$-$Fe_2O_3$ and $Sn^{4+}$-$Fe_2O_3$ films.

| | $O_L$ | | $O_V$ | |
|---|---|---|---|---|
| Samples | BE | At% | BE | At% |
| $Fe_2O_3$ | 529.63 | 51.50 | 531.44 | 48.50 |
| $Sn^{2+}$-$Fe_2O_3$ | 529.93 | 60.98 | 531.51 | 39.02 |

* *Corresponding authors. Email: wwxia@yzu.edu.cn; xhzeng@yzu.edu.cn*

| | | | | |
|---|---|---|---|---|
| $Sn^{4+}$-$Fe_2O_3$ | 529.47 | 43.35 | 531.38 | 56.65 |

Table S3. Comparison of PEC performance and morphology for different hematite reported previously.

| Material/ Reference | Electrolyte | IPCE (%) | Photocurrent density(mA/cm$^2$) | Annealing temperature/Time |
|---|---|---|---|---|
| Sn-$Fe_2O_3$ nanostructures[1] | 1M NaOH | 23.7 (1.4$V_{RHE}$) | 1.63 (1.4$V_{RHE}$) | 800℃/10min |
| E-I-Sn-$Fe_2O_3$ NWs[2] | 1M KOH | 27 (0.23$V_{Ag/AgCl}$) | 1.36 (0.23$V_{Ag/AgCl}$) | 800℃/20min (HF Etching $SiO_2$ encapsulation) |
| Sn-$Fe_2O_3$ nanocorals[3] | 1M NaOH | 19.8 (1.23$V_{RHE}$) | 1.86 (1.23$V_{RHE}$) | 800℃/20min |
| Sn-$Fe_2O_3$ [4] | 1M NaOH | 17 (1.23$V_{RHE}$) | 0.86 (1.23$V_{RHE}$) | 800℃/20min |
| Sn-$Fe_2O_3$ nanorod[5] | 1M NaOH | | 1.35 (1.23$V_{RHE}$) | 800℃/10min |
| Sn-$Fe_2O_3$ nanorod[6] | 1M NaOH | | 1.00 (1.23$V_{RHE}$) | 800℃/10min |
| Sn-$Fe_2O_3$ nanorod[7] | 1M KOH | 22 (1.23$V_{RHE}$) | 0.93 (1.23$V_{RHE}$) | 800℃/3min |
| Sn-$Fe_2O_3$ nanotubes[8] | 1M NaOH | | 0.65 (1.23$V_{RHE}$) | 750℃/30min |
| Sn-$Fe_2O_3$[9] | 1M NaOH | | 0.96 (1.23$V_{RHE}$) | 750℃/15min |
| Sn(8%)-$Fe_2O_3$[10] | 1M KOH | 9.9 (1.6$V_{RHE}$) | 0.298 (1.6$V_{RHE}$) | 600℃/240min |

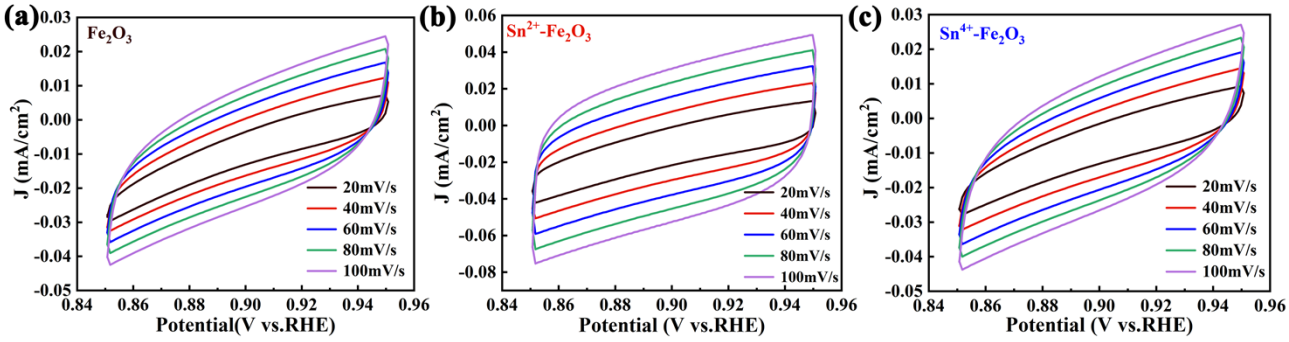


**Figure S2.** Cyclic voltammetry (CV) for $Fe_2O_3$, $Sn^{2+}$-$Fe_2O_3$ and $Sn^{4+}$-$Fe_2O_3$ photoanodes at various scan rates.

**Figure S3.** EIS Nyquist for $Fe_2O_3$, $Sn^{2+}$-$Fe_2O_3$ and $Sn^{4+}$-$Fe_2O_3$ photoanodes.

**Reference**

[1] A. Annamalai, P.S. Shinde, T.H. Jeon, H.H. Lee, H.G. Kim, W. Choi, J.S. Jang, Fabrication of superior α-Fe2O3 nanorod photoanodes through ex-situ Sn-doping for solar water splitting, Solar Energy Materials and Solar Cells, 144 (2016) 247-255.

[2] M. Li, Y. Yang, Y. Ling, W. Qiu, F. Wang, T. Liu, Y. Song, X. Liu, P. Fang, Y. Tong, Y. Li, Morphology and Doping Engineering of Sn-Doped Hematite Nanowire Photoanodes, Nano Letters, 17 (2017) 2490-2495.

[3] Y. Ling, G. Wang, D.A. Wheeler, J.Z. Zhang, Y. Li, Sn-Doped Hematite Nanostructures for Photoelectrochemical Water Splitting, Nano Letters, 11 (2011) 2119-2125.

[4] A.G. Tamirat, W.-N. Su, A.A. Dubale, H.-M. Chen, B.-J. Hwang, Photoelectrochemical water splitting at low applied potential using a NiOOH coated codoped (Sn, Zr) α-Fe2O3 photoanode, J. Mater. Chem. A, 3 (2015) 5949-5961.

[5] H. Ma, M.A. Mahadik, J.W. Park, M. Kumar, H.S. Chung, W.S. Chae, G.W. Kong, H.H. Lee, S.H. Choi, J.S. Jang, Highly self-diffused Sn doping in α-Fe2O3 nanorod photoanodes initiated from β-FeOOH nanorod/FTO by hydrogen treatment for solar water oxidation, Nanoscale, 10 (2018) 22560-22571.

[6] A. Annamalai, H.H. Lee, S.H. Choi, S.Y. Lee, E. Gracia-Espino, A. Subramanian, J. Park, K.-j. Kong, J.S. Jang, Sn/Be Sequentially co-doped Hematite Photoanodes for Enhanced Photoelectrochemical Water Oxidation: Effect of Be2+ as co-dopant, Scientific Reports, 6 (2016).

[7] J. Wang, C. Du, Q. Peng, J. Yang, Y. Wen, B. Shan, R. Chen, Enhanced photoelectrochemical water splitting performance of hematite nanorods by Co and Sn co-doping, Int. J. Hydrog. Energy, 42 (2017) 29140-29149.

[8] S.-F. Duan, Y.-Y. Geng, X.-B. Pan, X.-Q. Yao, Y.-X. Zhao, X. Li, C.-L. Tao, D.-D. Qin, Tubular morphology preservation and doping engineering of Sn/P-codoped hematite for photoelectrochemical water oxidation, Dalton Transactions, 48 (2019) 928-935.

[9] J. Cai, H. Chen, C. Liu, S. Yin, H. Li, L. Xu, H. Liu, Q. Xie, Engineered Sn- and Mg-doped hematite photoanodes for efficient photoelectrochemical water oxidation, Dalton Transactions, 49 (2020) 11282-11289.

[10] T.H. Jeon, H.-i. Cho, H. Park, H.-i. Kim, W. Choi, Synergistic effect of Sn doping and hydrogenation on hematite electrodes for photoelectrochemical water oxidation, Materials Chemistry Frontiers, 5 (2021) 6592-6602.